

The Investigation of SME in a Cu-Al-Ni HTSMA

O. Karaduman¹, N. Ünlü¹, C. Aksu Canbay^{1, a)}, İ. Özkul², S. Aziz Baiz¹

¹Department of Physics, Faculty of Science, Firat University, Elazig 23169, TURKEY

²Mersin University, Faculty of Engineering, Department of Mechanical Engineering, Mersin/TURKEY

When some alloys, called shape memory alloys (SMAs), are exposed to different physical external factors such as heat, pressure, magnetic field or their different combinations, they can give different behavioral responses and can be forced into microstructural changes called martensitic phase transformations in which only their crystal structures change, while the neighborhoods of the atoms remain constant. Due to their controllable macroscopic shape change abilities which arise from those transformations, both commercial uses and further explorative investigations of these alloys are continuing without slowing down. In this work, a Cu-Al-Ni shape memory alloy with a new chemical composition was fabricated by arc melting method. In order to dig up its prospective characteristic shape memory effect (SME) property, the alloy was investigated by thermal and structural analysis measurements. The differential thermal analysis measurements of the sample were made at different heating/cooling rates. The diffraction planes of the martensite structures in the alloy sample were determined by XRD at room temperature. The XRD results supported with optical micrograph observations. In conclusion, this chemically new composed CuNi alloy may be useful in various thermomechanical SMA applications.

Keywords: CuAlNi HTSMA, SME, Martensite, DTA, DSC, XRD, Optical microscopy

Submission date: 13 February 2018

Acceptance Date: 06 March 2018

*Corresponding author: caksu@firat.edu.tr

1. Introduction

If shape memory alloys are deformed when they are in martensite (M) phase (at low temperature phase), they can regain their first original predeformed shapes by heating up or some other physical effects. Generally, these alloys can be plastically deformed at low temperature and return to pre-deformed shapes at high temperatures. What causes this recall is a non-diffusive reversible transformation [1, 2]. With external forces they change into martensite phase or when they heated up they can convert into austenite (A) phase. These phases convertible to one another are characterized by their austenite start (A_s), austenite finish (A_f), martensite start (M_s) and martensite finish (M_f) temperatures and the values of these temperatures have a relationship between each other as $M_f < M_s < A_s < A_f$ [3]. From starting at M_s temperature the martensitic transformation occurs continuously and increasingly as the temperature decreases, then it will be all completed at M_f and thus such a thermoelastic martensitic transformation takes place [4].

Among the shape memory alloys, copper-based ones are preferred due to their low costs and easy production process. Binary Cu-based SMAs are mostly classified in three

basic groups. These are Cu-Zn, Cu-Al and Cu-Sn as shown in the Fig.1. These binary alloys are often doped with one or more elemental additive contents for bringing in them phase stability, more ductility (by grain refinement), higher or lower transformation temperatures ranges or some other demanded special properties.

At high temperatures and by about 12%wt Al content, a bcc lattice structure of β phase will occur in all Cu-rich matrix as shown in Fig.2. By a slow cooling down, this β phase separates into the phases of γ_2 and α phase (fcc) at around 838 K by eutectoid separation. If the alloy is cooled rapidly from the β phase region, the eutectoid decomposition is inhibited and the martensite transformation occurs at temperatures below the M_s temperature. When the concentration of Al is higher than 11%wt, the irregular β phase is converted into the regular β_1 phase ($DO_3(L2_1)$ type superlattice structure) [5, 6].

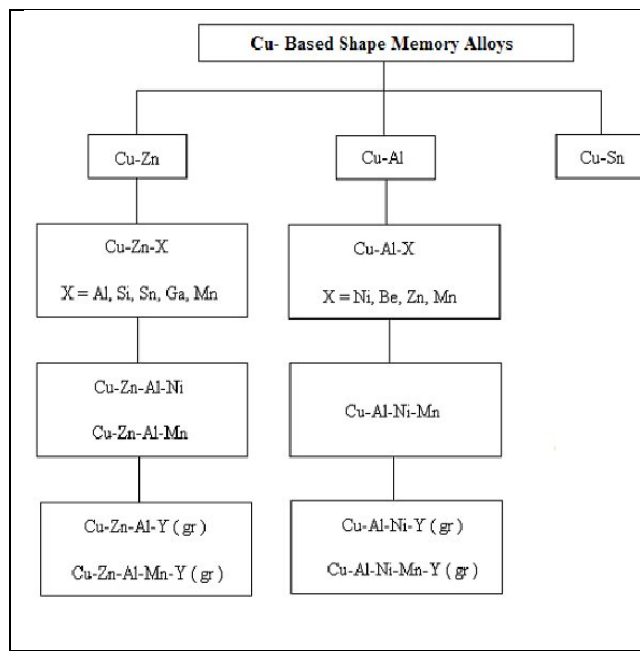


Fig.1: Cu-based shape memory alloys. Y(g) elements can be Ti, Co, Zr, Mn, V, Ce and B elements and are used for grain refinement [7, 8].

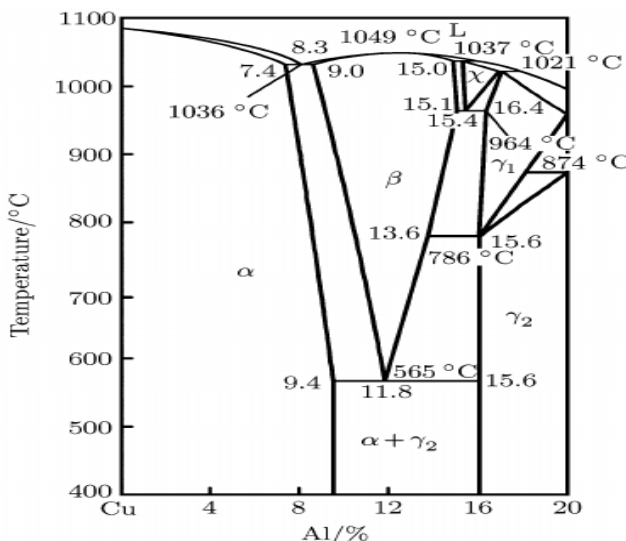


Fig.2: Binary phase diagram of CuAl alloy [9].

The main goal of this study was to examine the existence of shape memory effect property in newly composed Cu-Al based shape memory alloy. For this, the characterization processes were carried out by thermal and structural measurements and analyses.

2. Experimental details

High purity elements of copper, aluminum and nickel (99.9%) powders were used to produce the ternary Cu-based polycrystalline shape memory alloy. After making pelletization under pressure, the alloy was fabricated by Edmund Buehler Arc Melter. The alloy was obtained as cast ingot and the minuscule specimens were cut from this ingot then these were solution-treated in β - phase region and

without delay quenched into iced-brine water to make the formation of β_1' martensite phase in them. The chemical composition of the fabricated alloy was determined by Bruker Model energy dispersive X-Ray analysis and was given in Table 1. The characteristic thermoelastic martensitic transformation data were obtained by differential thermal analysis (DTA) measurements with the running temperature rates of 5, 15, 25 and 35 °C/min. X-Ray measurements (with CuK α radiation) were performed by a Rigaku RadB-DMAX II diffractometer at room temperature to determine the lattice diffraction planes of the alloy. The optical metallography observations were also made at room temperature to detect the martensite formations on the surface of the alloy sample.

Table 1: Chemical composition of CuAlNi alloy.

Elements	Chemical Composition (at %)
Cu	69.65
Al	25.64
Ni	4.71

3. Results and discussion:

The DTA heating and cooling loop curves of the CuAlNi alloy can be seen in Fig.3. The characteristic transformation temperatures and enthalpy values of the alloy were determined by peak analyses of these curves. These thermal measurements were taken from room temperature to 950 °C with different heating/cooling (h/c) rates of 5, 15, 25 and 35 °C/min. By using the data obtained from DTA, the values of transformation hysteresis ($A_s - M_f$) and some thermodynamic parameters were calculated for each heating/cooling rate and were given in Table 2. Among these thermodynamic parameters, the equilibrium temperature (T_0) was calculated by using the following equation [10] below;

$$T_0 = \frac{1}{2} (M_s + A_f) \quad (1)$$

Another thermodynamic parameter is lattice vibrational entropy change throughout martensitic transformation and it was calculated (for M to A phase transition) by the formula [11] following as;

$$\Delta S_{M \rightarrow A} = \Delta H_{M \rightarrow A} / T_0 \quad (2)$$

As the heating/cooling rate changed, the transformation temperatures were changed slightly, as seen in Table 2 and Fig.3. On the left side of heating parts of the cycles, the first downward endothermic peaks (called austenite peaks) belong to the forward M \rightarrow A transformation (at $\sim 400-450$ °C) where β_1' converts to $\beta_1(L2_1)$ phase. On the right side of these peaks there exist small endothermic peaks of $\beta_1 \rightarrow \beta_2$ (metastable) and these are followed cheek by jowl by the bigger exothermic peaks of $\beta_2 \rightarrow \alpha + \gamma_2$

separations which are able to be seen more clearly on the curves of 25 and 35 °C/min heating rates. Then these α and γ_2 phases dissolve and convert to a stable ordered β_2 phase that can be understood from the downward eutectoid dissolution peaks at around 620 °C. All this multi-stage

understood that these two parameters are directly proportional and the drawn graphs became compatible with this equation [16].

Table 2: Transformation temperatures and kinetic parameters of the CuAlNi sample at different heating/cooling rates.

Rate (°C/min)	A_s (°C)	A_f (°C)	A_{max} (°C)	T_o (°C)	$\Delta H_{M \rightarrow A}$ (J/g)	$\Delta S_{M \rightarrow A}$ (J/g°C)	M_s (°C)	M_f (°C)	$A_s - M_f$ (°C)	$A_f - M_s$ (°C)
5	402,44	426,34	408,82	342,75	0,49	0,0014	258,61	230,14	172,30	167,73
15	402,44	425,49	408,82	344,62	0,51	0,0015	263,75	240,14	162,30	161,74
25	402,12	457,84	423,58	358,46	8,13	0,0226	259,08	236,18	165,94	198,76
35	402,34	453,40	429,47	354,60	5,45	0,0153	255,81	234,41	167,93	197,59

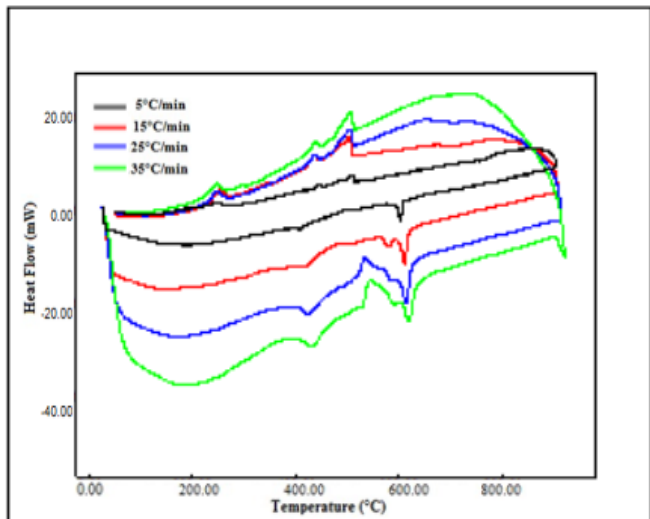


Fig.3: DTA curves of the sample obtained at different heating/cooling rates (5, 15, 25 and 35 °C/min).

transitions process reversed back on the cooling parts of the curves. The cooling down phase transitions in Cu-based shape memory alloys usually take place in three stages; $A_2 \rightarrow B_2 \rightarrow DO_3$ (or L_2) $\rightarrow \beta_1'$ (9R, 18R or 18R+2H). The reverse $A \rightarrow M$ phase transition peaks (martensite peaks) positioned at about 250-270°C.

In this study, the characteristic martensitic transformation temperature of Cu-25.64Al-4.71Ni (at%) alloy sample was detected as 259.08 °C and this value is higher than that of some previously reported CuAlNi alloys [12-14]. The reason for this is that the martensitic transformation temperature decreases by increasing the content of Al element in Cu-based alloys [15], using a higher Cu and lower content of Al here led to an increase in the transformation temperature.

Fig.4 shows the entropy and enthalpy changes versus heating/cooling rate and their graphics both remained parallel and close to each other all the while. They stayed unvaried between 5 and 15 °C/min of heating/cooling rates.

But at between 15-35 °C/min of heating rates they both at first increased and then decreased. According to Eq.2, it is easily

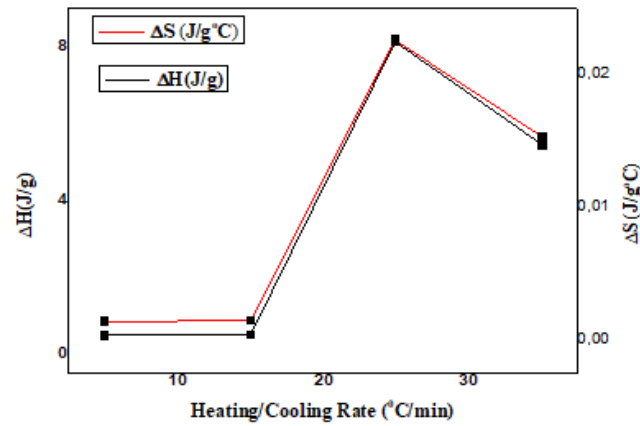


Fig.4: The enthalpy and entropy change plots of CuAlNi alloy versus heating/cooling rate.

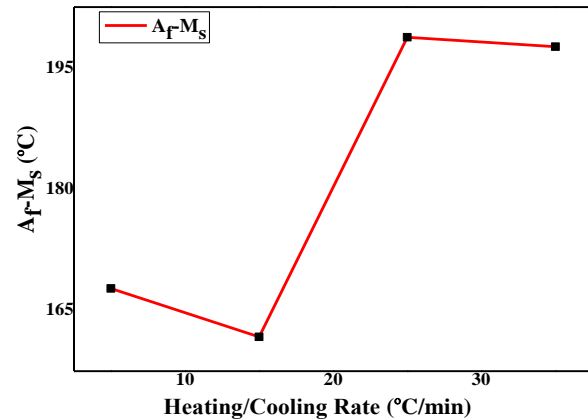


Fig.5: Variation of transformation hysteresis switches by heating/cooling rate.

The reversible transformations exhibit a thermoelastic property determined by hysteresis temperature range. By increase of heating/cooling rate according to the Fig.5, it is also possible to say that the $A_f - M_s$ temperature range values are increased [17].

Optical microscopy was used to analyze the structural surface morphology of the sample and the obtained micrographs are presented in Fig.6. Since the surface images of the alloy sample were taken at room temperature, the alloy should be in martensite phase, therefore these micro-optical images displayed martensite forms on the surface of the sample. It was determined that these morphological structure forms belong to V and needle type of $\beta 1'$ ($\beta 3'$) phase and some $\gamma 1'$ ($\gamma 3'$) plates of martensite forms [18].

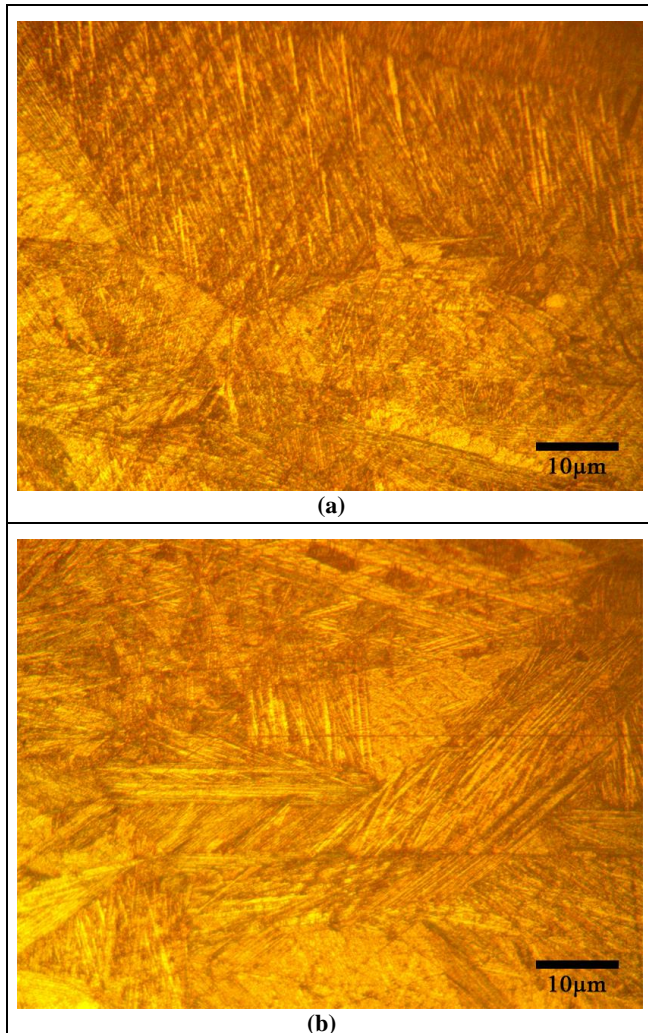


Fig.6: Two different optical micrograph shots on the morphological surface of the CuAlNi sample at room temperature.

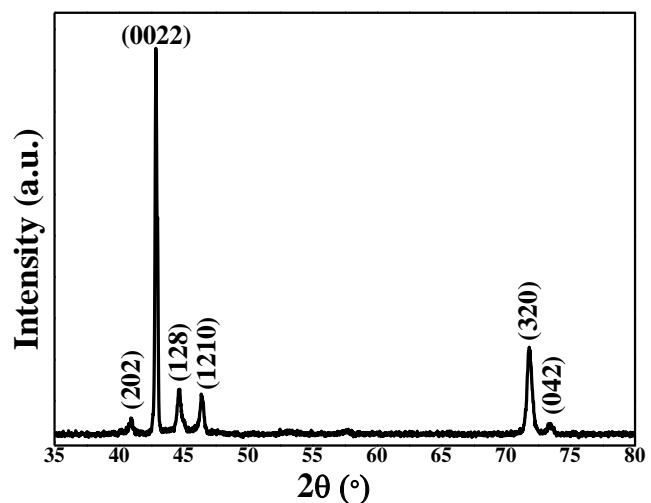


Fig.7: X-Ray diffraction peaks and correspondent martensite planes of the CuAlNi alloy.

The crystallographic structural analysis of the alloy sample was made by X-Ray diffraction technique at room temperature and Fig.7 shows the X-Ray diffraction pattern of the available phases which diffracted the incident x-rays. From the pattern it is understood that the alloy has a monoclinic crystal structure. The highest peak of (0022) plane and the other characteristic (202), (128), (1210), (320) and (042) planes are all belong to $\beta 1'$ phase martensite forms and are similar to the previous reports [19-23]. X-Ray analysis results provided consistency with thermal analysis and optical micrograph results.

Conclusions

Micro-structural aspects and thermodynamic parameters of Cu-25.64Al-4.71Ni at% shape memory alloy were brought to light. Main phase in the alloy sample was observed to have monoclinic 18R martensite structure at room temperature by X-ray diffraction method. This result became consistent with the optical micrographs of the alloy taken at room temperature. The DTA analysis revealed the phase transition sequence of $B2 \rightarrow \beta 1(L_{21}) \rightarrow \beta 1'(18R+2H)$ under cooling process, which is common to CuAlNi SMAs and the characteristic martensitic transformation temperature of the alloy sample was detected as 259.08 °C, thereby the alloy was took in HTSMA class. The calculated enthalpy and entropy values (during the transition from martensite to austenite) are generally increased with increasing heating/cooling rate. All the results of this study indicated that this new CuAlNi shape memory alloy composition system may be useful in various high temperature applications in which its appropriate shape memory effect and thermomechanical properties are needed.

Acknowledgements

This study was financially supported by the Research Fund of Mersin University in Turkey with the project number 2018-1-AP1-2839.

References:

[1] D. Hartl, D. Lagoudas, Aerospace applications of shape memory alloys, Proceedings of the Institution of Mechanical Engineers, Part G: Journal of Aerospace Engineering, SAGE, (2007), pp. 535-552.
<https://doi.org/10.1243/09544100JAERO211>

[2] A. Nespoli, S. Bessegini, S. Pittaccio, E. Villa, S. Viscuso, The high potential of shape memory alloys in developing miniature mechanical devices: A review on shape memory alloy mini-actuators, *Sensor Actuat. A-Phys.* 158 (1) (2010) 149-160.
<https://doi.org/10.1016/j.sna.2009.12.020>

[3] Rahman, M.A., Recent Patents on Mech. Eng., 1(2008), 65-67.

[4] Zhang, S., McCormick, P.G., *Acta Mater.* 48(2000), 3081-3089.
[https://doi.org/10.1016/S1359-6454\(00\)00120-8](https://doi.org/10.1016/S1359-6454(00)00120-8)

[5] Miyazaki, S. ve Otsuka, K., "Development of Shape Memory Alloys", *ISIJ International*, 29(5): 353-377 (1989).
<https://doi.org/10.2355/isijinternational.29.353>

[6] Otsuka, K. et al., "Structure Analysis of Stres-Induced β_1 " Martensite in a Cu-Al-Ni Alloy by Neutron Diffraction", *Acta Metall.*, 27: (1979), 965-972.
[https://doi.org/10.1016/0001-6160\(79\)90184-6](https://doi.org/10.1016/0001-6160(79)90184-6)

[7] Balo, Ş.N., 'The Investigation of Shape memory Properties of Cu-A-Be and Cu-Al-Ni Alloys by Mechanical Effects', PhD. Thesis, Department of Physics, Institutue of Science, Elazığ/Turkey(In Turkish), 1999.

[8] R. Dasgupta, A look into Cu-based shape memory alloys: Present scenario and future prospects, *J. Mater. Res.*, Vol. 29, No. 16 (2014), pp. 1681-1689.
<https://doi.org/10.1557/jmr.2014.189>

[9] Massalski T.B. et al., *Binary Alloy Phase Diagrams*, Metals Park OH: Ameri-can Society for Metals (1986), 2 volumes: pp. xiii- 2224.

[10] Kurt, B., Orhan, N., "Şekil Hafızalı Alaşımların Kullanım Alanları Üzerine Son Gelişmeler", Denizli Malzeme Sempozyumu PAÜ-Mühendislik Fakültesi Denizli, (2002), p 459-465.

[11] Akdoğan, A. ve Nurveren, K., Akıllı Malzemeler ve Uygulamaları, Machinery MakinaTek, sayı 57, (2002) s. 35.

[12] Karagoz, Z. & Canbay, C.A. *J Therm Anal Calorim* (2013) 114: 1069.
<https://doi.org/10.1007/s10973-013-3145-9>.

[13] K. Akash et al., Parametric investigations to enhance the thermomechanical properties of CuAlNi shape memory alloy Bi-morph, *Journal of Alloys and Compounds* 720 (2017) 264e271
<https://doi.org/10.1016/j.jallcom.2017.05.255>

[14] S.M. Chentouf et al., *Journal of Alloys and Compounds* 470 (2009) 507-514.
<https://doi.org/10.1016/j.jallcom.2008.03.009>

[15] Akdoğan, A. ve Nurveren, K., Akıllı Malzemeler ve Uygulamaları, Machinery MakinaTek, sayı:57 (2002), s. 35.

[16] R.J. Salzbrenner, M. Cohen, *Acta Metall.* 27, (1979), 739.
[https://doi.org/10.1016/0001-6160\(79\)90107-X](https://doi.org/10.1016/0001-6160(79)90107-X)

[17] C. Aksu Canbay, A. Aydogdu, *J. Therm. Anal. Calorim.* 113, 731 (2012).
doi:10.1007/s10973-012-2792-6

[18] Recarte, V., Pérez-Sáez, R.B., San Juan, J. et al. *Metall and Mat Trans A* (2002) 33: 2581.
<https://doi.org/10.1007/s11661-002-0379-8>

[19] Braga et al., *Materials Research*, 20(6) (2017): 1579-1592.
DOI:<http://dx.doi.org/10.1590/1980-5373-MR-2016-0476>

[20] S.N. Saud et al., *Journal of Materials Engineering and Performance*, 24 (2015):1522-1530.
DOI:[10.1007/s11665-015-1436-y](https://doi.org/10.1007/s11665-015-1436-y)

[21] C.A. Canbay et al., *Physics of Metals and Metallography*, Vol. 119, No. 6, (2018), pp. 536-541.
<https://doi.org/10.1134/S0031918X18060030>

[22] S.N. Saud et al., *J. Mater. Res.*, Vol. 30, No. 14 (2015), p.2262.
DOI:[10.1557/jmr.2015.196](https://doi.org/10.1557/jmr.2015.196)

[23] I. Ozkul et al., *Russian Journal of Non-Ferrous Metals*, Vol. 58, No. 2, (2017), pp. 130-135.
DOI: [10.3103/S1067821217020092](https://doi.org/10.3103/S1067821217020092)